

# The Cramér–Rao Bound for Pole and Amplitude Coefficient Estimates of Damped Exponential Signals in Noise

William M. Steedly, *Member, IEEE*, and Randolph L. Moses, *Senior Member, IEEE*

**Abstract**—This paper provides a complete Cramér–Rao bound (CRB) derivation for the case where signals consist of arbitrary exponential terms in noise. Expressions for the CRB's of the parameters of a damped exponential model with one set of poles and multiple sets of amplitude coefficients are derived. CRB's for the poles and amplitude coefficients are derived in terms of both rectangular and polar coordinate parameters. In rectangular parameters it is shown that the real and imaginary part CRB's for both the poles and amplitude coefficients are equal and uncorrelated. In polar coordinates the angle and magnitude CRB's are also uncorrelated; furthermore, the CRB's of the pole angles and relative magnitudes are equal, and are logarithmically symmetric about the unit circle.

## I. INTRODUCTION

THE problem of estimating model parameters of noisy exponential signals is an active area of research. These models have a single set of complex poles and one or more set of amplitude coefficients (snapshots). The performance of these parameter estimation methods is often measured by the accuracy of the estimated poles, since these pole locations contain such information as formant frequencies or directions of arrival of signal components. This problem is considered in [1] and estimators are derived for the case where the poles are confined to lie on the unit circle. To evaluate the accuracy of the estimators, a general expression for the Cramér–Rao bounds (CRB's) are derived for the real and imaginary parts of the amplitude coefficients and the pole angles under the assumption that the poles of the signal lie on the unit circle. In [2] and [3] the signal snapshot case is considered and the CRB's are derived for magnitude and angle parameters of the amplitude coefficients and poles.

This paper provides a complete CRB derivation for the multi-snapshot case where signals consist of arbitrary exponential terms in noise. Such models are used in a broad range of problems, including speech processing, decon-

volution, radar and sonar signal processing, array processing, and spectrum estimation [4]–[15]. Thus, it is of interest to obtain expressions for the CRB's of this model. CRB's for the poles and amplitude coefficients are derived in terms of both rectangular and polar coordinate parameters. CRB's are also derived assuming that relative magnitudes of pole and amplitude coefficients are estimated, rather than absolute magnitudes.

Using these expressions, it is shown that for the rectangular parameters the real and imaginary part CRB's for both the poles and amplitude coefficients are equal and uncorrelated. It is also shown that for the polar parameters the angle and magnitude CRB's are uncorrelated, but in general unequal. However, the CRB of the relative magnitude of the pole or amplitude coefficient estimate (i.e.,  $\hat{\alpha}/\alpha$ , where  $\alpha$  is the true magnitude) is equal to the CRB of the angle estimate of that parameter. It is also shown that some of the CRB's are independent of the absolute phase of the set of poles and each set of amplitude coefficients.

This paper also examines pole estimation accuracy as functions of pole magnitude, data length, and pole separation using the CRB expressions. It is shown that for small data lengths, poles slightly inside the unit circle are more accurately estimated than poles on the unit circle. In addition, the transition from the  $1/m^3$  (where  $m$  is the number of data points) variance bounds decrease for poles on the unit circle to the variance decrease as poles move off the unit circle is also detailed.

An outline of this paper is as follows. In Section II the multi-snapshot data model is presented. Section III presents the CRB covariance matrices and their properties. Section IV presents some examples using the CRB expressions. Finally, the Section V concludes the paper.

## II. DATA MODEL

Assume we have  $N$  “snapshots” of data vectors  $y(t)$ , each of length  $m$ :

$$y(t) = [y_0(t) \ y_1(t) \ \cdots \ y_{m-1}(t)]^T$$

$$t = 1, 2, \cdots, N. \quad (1)$$

Each data vector is modeled as a noisy exponential se-

Manuscript received February 7, 1991; revised March 20, 1992. This work was supported in part by the Air Force Office of Scientific Research, Bolling AFB, DC, and in part by the Avionics Division, Wright Laboratories, Wright Patterson AFB, Ohio.

W. M. Steedly was with the Department of Electrical Engineering, Ohio State University, Columbus, OH 43210. He is now with the Analytic Sciences Corporation, Reston, VA 22090.

R. L. Moses is with the Department of Electrical Engineering, Ohio State University, Columbus, OH 43210.

IEEE Log Number 92060402.





where

$$\begin{aligned} U(t) &= \frac{2}{\sigma} X^H(t) A^H A X(t) \\ V(t) &= \frac{2}{\sigma} X^H(t) A^H C A X(t) \\ W &= \frac{2}{\sigma} \sum_{t=1}^N X^H(t) A^H C C A X(t) \end{aligned} \quad (14)$$

and where  $T_\alpha$  and each  $T_\beta(t)$  are diagonal matrices given by

$$\begin{aligned} T_\alpha &= \text{diag} \left( \frac{1}{\alpha_1}, \frac{1}{\alpha_2}, \dots, \frac{1}{\alpha_n} \right) \\ T_\beta(t) &= \text{diag} \left( \frac{1}{\beta_1(t)}, \frac{1}{\beta_2(t)}, \dots, \frac{1}{\beta_n(t)} \right). \end{aligned} \quad (15)$$

The corresponding CRB covariance matrix is given by

$$\text{CRB}_\theta^{\text{pol}} = \begin{bmatrix} \frac{\sigma^2}{mN} & & & & & & \\ & \bar{U}'(1, 1) & \bar{U}'(1, 1) T_\beta^{-1}(1) & \dots & \bar{U}'(1, N) & \bar{U}'(1, N) T_\beta^{-1}(N) & \bar{V}'(1) & \bar{V}'(1) T_\alpha^{-1} \\ & -T_\beta^{-1}(1) \bar{U}'(1, 1) & T_\beta^{-1}(1) \bar{U}'(1, 1) T_\beta^{-1}(1) & \dots & -T_\beta^{-1}(1) \bar{U}'(1, N) & T_\beta^{-1}(1) \bar{U}'(1, N) T_\beta^{-1}(N) & -T_\beta^{-1}(1) \bar{V}'(1) & T_\beta^{-1}(1) \bar{V}'(1) T_\alpha^{-1} \\ & \vdots & \vdots & \ddots & \vdots & \vdots & \vdots & \vdots \\ & \bar{U}'(N, 1) & \bar{U}'(N, 1) T_\beta^{-1}(1) & \dots & \bar{U}'(N, N) & \bar{U}'(N, N) T_\beta^{-1}(N) & \bar{V}'(N) & \bar{V}'(N) T_\alpha^{-1} \\ & -T_\beta^{-1}(N) \bar{U}'(N, 1) & T_\beta^{-1}(N) \bar{U}'(N, 1) T_\beta^{-1}(1) & \dots & -T_\beta^{-1}(N) \bar{U}'(N, N) & T_\beta^{-1}(N) \bar{U}'(N, N) T_\beta^{-1}(N) & -T_\beta^{-1}(N) \bar{V}'(N) & T_\beta^{-1}(N) \bar{V}'(N) T_\alpha^{-1} \\ & \bar{V}''(1) & \bar{V}''(1) T_\beta^{-1}(1) & \dots & \bar{V}''(N) & \bar{V}''(N) T_\beta^{-1}(N) & \bar{W}' & \bar{W}' T_\alpha^{-1} \\ & -T_\alpha^{-1} \bar{V}''(1) & -T_\alpha^{-1} \bar{V}''(1) T_\beta^{-1}(1) & \dots & -T_\alpha^{-1} \bar{V}''(N) & -T_\alpha^{-1} \bar{V}''(N) T_\beta^{-1}(N) & -T_\alpha^{-1} \bar{W}' & -T_\alpha^{-1} \bar{W}' T_\alpha^{-1} \end{bmatrix} \quad (16)$$

where

$$\begin{aligned} U'(t, s) &= U^{-1}(t) \delta_{t,s} + U^{-1}(t) V(t) W' V^H(s) U^{-1}(s) \\ V'(t) &= -U^{-1}(t) V(t) W' \\ W' &= \frac{\sigma}{2} \left( \sum_{t=1}^N X^H(t) A^H C P_{AX}^\perp(t) C A X(t) \right)^{-1} \\ P_{AX}^\perp(t) &= I_m - A X(t) (X^H(t) A^H A X(t))^{-1} X^H(t) A^H. \end{aligned} \quad (17)$$

*Proof:* See Appendix B.

*Corollary 2:* In  $\text{CRB}_\theta^{\text{pol}}$ ,  $\text{cov}(\hat{\gamma}_i(t), \hat{\beta}_i(t)) = 0$ , and  $\text{cov}(\omega_i, \alpha_i) = 0$ .

*Proof:* The corresponding cross terms in  $\text{CRB}_\theta^{\text{pol}}$  are the diagonal elements of the product of the imaginary part

of a Hermitian matrix and a diagonal matrix and are thus identically zero.  $\square$

Note the similarity between the Fisher information matrices and CRB matrices for the rectangular and polar parameterizations. These matrices have the same structure except for the presence of the  $T_\alpha$  and  $T_\beta(t)$  diagonal matrices. Accordingly, the cross terms in the CRB for the parameter pairs of each amplitude coefficient and of each pole are zero for both formulations as expressed by Corollaries 1.a and 2. Note that with the polar parameterization, the variance CRB's of the two parameters in each pair are not equal as they are with the rectangular parameterization.

We can obtain all of the structure present with the rectangular parameterization by an appropriate normalization of the polar parameters. Consider estimates of the relative magnitudes of the poles and amplitude coefficients as fol-

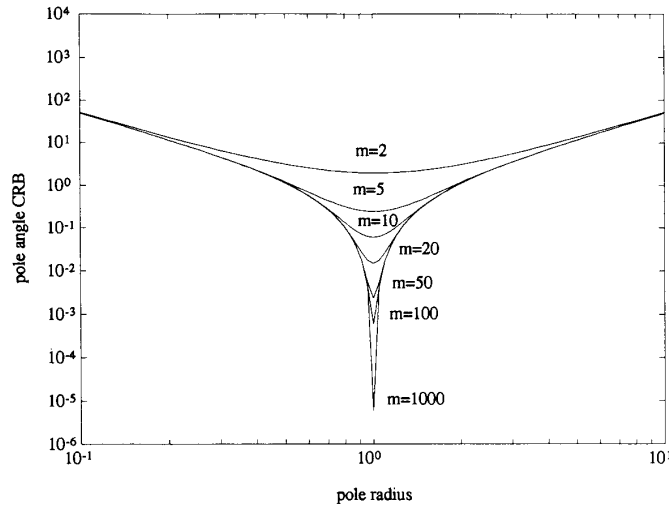
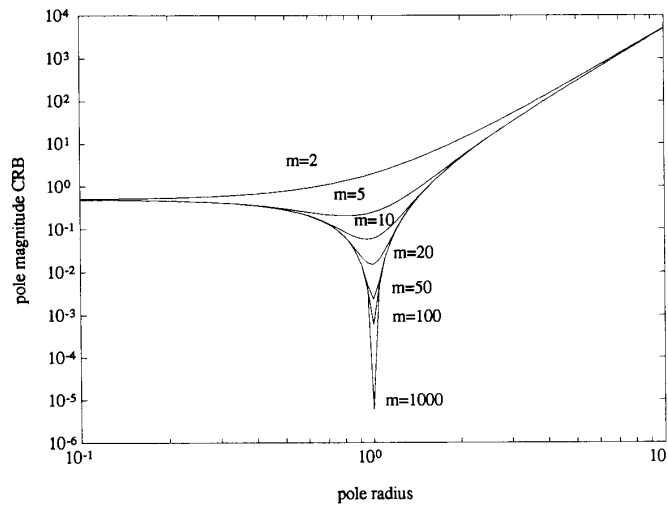
lows:

$$\begin{aligned} \hat{\theta}_x^{\text{relpol}} &= [\hat{\gamma}^T(1) \hat{\beta}^T(1) T_\beta(1) \hat{\gamma}^T(2) \hat{\beta}^T(2) T_\beta(2) \\ &\quad \dots \hat{\gamma}^T(N) \hat{\beta}^T(N) T_\beta(N)]^T \\ \hat{\theta}_p^{\text{relpol}} &= \left[ \hat{\omega}_1 \hat{\omega}_2 \dots \hat{\omega}_n \frac{\hat{\alpha}_1}{\alpha_1} \frac{\hat{\alpha}_2}{\alpha_2} \dots \frac{\hat{\alpha}_n}{\alpha_n} \right]^T \\ \hat{\theta}^{\text{relpol}} &= [\sigma \hat{\theta}_x^{\text{relpol}T} \hat{\theta}_p^{\text{relpol}T}]^T. \end{aligned} \quad (18)$$

By considering the polar parameterization with a relative magnitude parameter which is estimated rather than the absolute magnitude parameter we obtain the parameter pair CRB equivalence of the rectangular parameterization.

*Theorem 3:* Assume we are given data as defined by (1) and (2). Then the Fisher information matrix for the



Fig. 1. Pole angle and CRB for single pole data ( $n = 1$ ).Fig. 2. Pole magnitude and CRB for single pole data ( $n = 1$ ).

angle of zero was chosen) from 0.1 to 10 and calculating the CRB using (11), (16), or (20) for data sets of lengths 2, 5, 10, 20, 50, 100, and 1000. For comparative purposes, the amplitude coefficient associated with the pole was chosen to be a positive real number such that the mode energy ( $x^2 \sum_{l=0}^{m-1} p^{2l}$ ) was unity for each pole location and data length. The noise power was also kept constant at  $\sigma = 1$ .

1) *Pole Location CRB*: The CRB for the pole angle and magnitude appears in Figs. 1 and 2, respectively. From Fig. 1 we see that the pole angle CRB is logarithmically symmetric with respect to the unit circle. The pole magnitude variance (Fig. 2) is not symmetric, and smallest at a pole radius less than one. However, the variance of the relative magnitude of the pole is and in fact is equal to the angle CRB in Fig. 1 (cf. Corollary 3.a). The fact

that these bounds are logarithmically symmetric is intuitively appealing, because reversing a data sequence would invert the pole, but should not affect its CRB.

From these two figures we see that inside the unit circle the CRB for pole angle is higher than the CRB for pole magnitude and vice versa outside the unit circle. This is due to the fact that angular uncertainty becomes greater as a pole moves closer to the origin. Note that the pole angle variance approaches infinity as the pole approaches the origin, which is what one would expect since its angle is undefined at the origin.

We see that the CRB for both pole angle and magnitude are asymptotically (as  $m \rightarrow \infty$ ) lowest when the pole is on the unit circle, and that on the unit circle the CRB is decreasing by  $1/m^2$  ( $m$  is the data length). This is consistent with the well-known  $1/m^3$  variance decrease, since

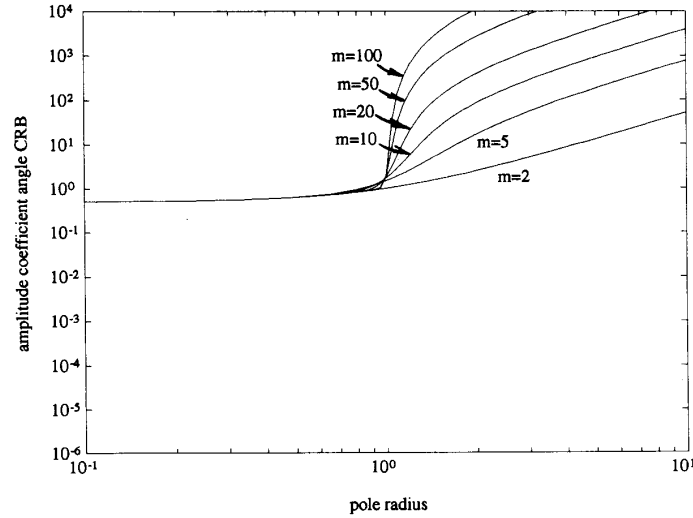


Fig. 3. Amplitude coefficient angle CRB for single pole data ( $n = 1$ ).

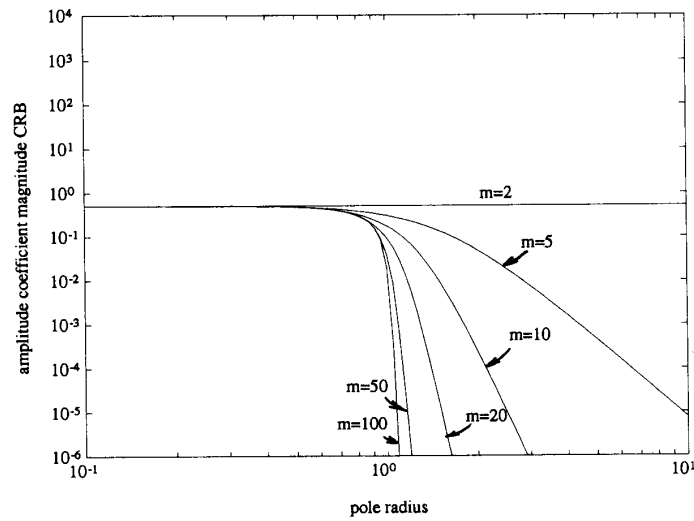


Fig. 4. Amplitude coefficient magnitude CRB for single pole data ( $n = 1$ ).

the amplitude coefficient was adjusted in this experiment to keep the mode energy constant (if the amplitude coefficient is left unchanged, the variance decrease is  $1/m^3$ ). The variance of the pole magnitude also exhibits a sharp decrease for poles near the unit circle, and for  $\alpha = 1$  has the same  $1/m^3$  variance decrease as is seen for pole angle. Note, however, that as the number of data points is reduced, the pole magnitude which gives the minimum CRB is less than unity.

When the pole is not on the unit circle, the CRB does not decrease to zero as  $m \rightarrow \infty$ . Because of the decay or growth of the exponential mode, and because the mode energy is kept constant, increasing  $m$  results in adding data points with lower and lower amplitude. Thus, the CRB does not continue to decrease. As a result, only a

finite amount of data is needed to obtain estimation accuracy which is nearly that of the infinite data case (for example, with a pole radius 0.8 the CRB's for pole angles and magnitudes for  $m = 20$  are essentially the same as those for  $m = \infty$ ).

2) *Amplitude Coefficient CRB*: The CRB for the amplitude coefficient angle and magnitude appear in Figs. 3 and 4. As before, each curve is a plot of CRB versus pole magnitude for a given number of data points.

There are several points to note in these figures. First, when the pole is inside the unit circle, increasing the number of data points provides no decrease in the bounds. Note that the first data point is precisely the amplitude coefficient; for a pole well inside the unit circle, by keeping the energy constant we keep the amplitude nearly con-

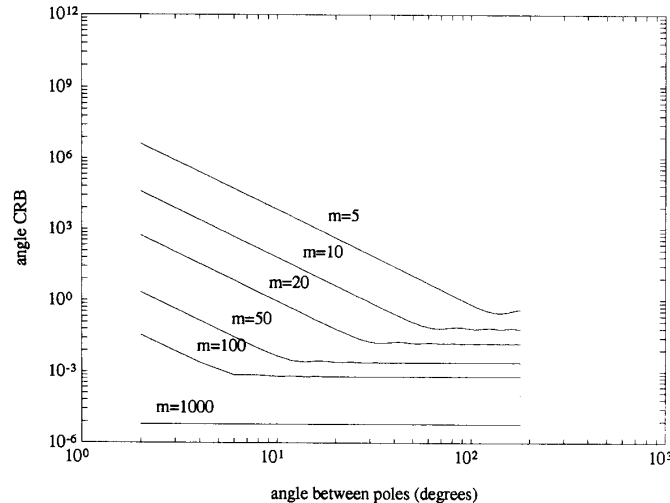


Fig. 5. Angle CRB as a function of pole separation for two poles on the unit circle.

stant. Outside of the unit circle the magnitude bounds drop dramatically as the number of data points is increased. At high growth rates, the first data point (which is the amplitude coefficient), is nearly zero, since the energy is held constant. Thus, the estimate of the amplitude cannot be expected to vary much around zero. This also causes the bounds for the angle to increase infinitely, due to angular uncertainty about zero as before with the pole angle.

Note that the CRB for the relative magnitude of the amplitude coefficient (i.e., the CRB of  $\hat{\beta}(1)/\beta(1)$ ) is given by Fig. 3 (cf. Corollary 3.a). Unlike the relative pole magnitude, this curve is not logarithmically symmetric with respect to the unit circle. The reason for this is that the amplitude coefficient is the first data point; flipping the sequence would correspond to having the CRB of the last data point, which is not the same as the CRB of the amplitude coefficient of a data sequence with an inverted pole. If one compares the CRB of the first data point of, say the sequence  $\{3(0.9)^q\}_{q=0}^{m-1}$  to the CRB of the last data point of the flipped sequence  $\{(3 \times 0.9^{m-1})(0.9)^q\}_{q=0}^{m-1}$ , one finds that they are equal, as they must be. Note that the amplitude coefficient was not merely inverted when the data sequence was flipped.

### B. Angle Separation

In the following simulations we consider two poles at  $\alpha_1 e^{j(\omega_0 + \Delta\omega/2)}$  and  $\alpha_2 e^{j(\omega_0 - \Delta\omega/2)}$  for various data lengths ( $m = 5, 10, 20, 50, 100, \text{ and } 1000$ ) and angle separation  $\Delta\omega$ . Note that without loss of generality we chose  $\omega_0 = 0$ ; the CRB's are invariant to  $\omega_0$  by Corollary 4. Again,  $\sigma = 1$ , one snapshot of data was used ( $N = 1$ ), and each amplitude was chosen such that the mode energy was unity.

1) *Angle Separation for Two Poles on the Unit Circle:* In this subsection we present results for  $\alpha_1 = \alpha_2 = 1$  (i.e., two poles located on the unit circle). Fig. 5

shows the CRB for the angle of either pole versus pole separation (the CRB are equal for the two poles) and for the various number of data points. The CRB for the pole magnitudes are equal to the pole angle CRB because these poles are located on the unit circle. These results are consistent with those in [16].

2) *Separation for Two Poles Inside the Unit Circle:* In the following simulation we consider two poles inside the unit circle. The poles have magnitudes of  $\alpha_1 = 0.85$  and  $\alpha_2 = 0.95$ . The CRB for each pole angle appear in Figs. 6 and 7 for the various data lengths. The CRB for each pole magnitude is proportional to the angle CRB, as was pointed out in the single pole simulation above.

From these figures we can see that the bounds exhibit the same type of characteristics as those in the experiment with two poles on the unit circle. One major difference is that as  $\Delta\omega \rightarrow 0$  the bounds remain finite, because the poles are at different radii, and thus never lie on top of one another. We note that for  $\Delta\omega = 0$ , we obtain CRB results for the case of real exponentials; this gives CRB results for the estimation problem considered in [17].

For large angle separations, the CRB's are relatively flat, and these bounds are higher than those for two poles on the unit circle. This is due to the fact that the angle CRB increases as a pole moves inside the unit circle, as was shown in Fig. 1 for the single pole case. The magnitude CRB exhibits the same relationship for the higher number of data points. However, for  $m = 5$  (and  $m = 10$  for  $p_2$ ) they were slightly lower than in Fig. 1, because locations of the minimum CRB for the pole magnitude are not always on the unit circle. (see Fig. 2).

As the data length increases, the CRB curves approach a lower limit because the poles lie off of the unit circle, as was observed in the single pole case. Thus, after  $m$  becomes sufficiently large ( $m \approx 100$  for the example shown), the addition of data does not appreciably lower the CRB.



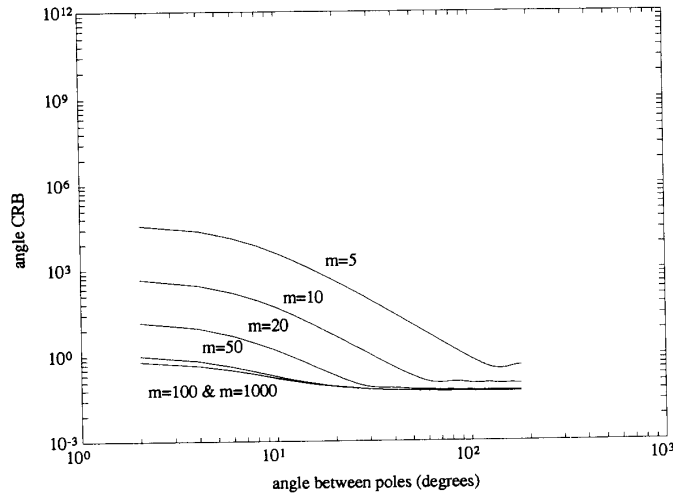


Fig. 6. Angle CRB for pole  $p_1$  as a function of angle separation, when  $\alpha_1 = 0.85$ ,  $\alpha_2 = 0.95$ .

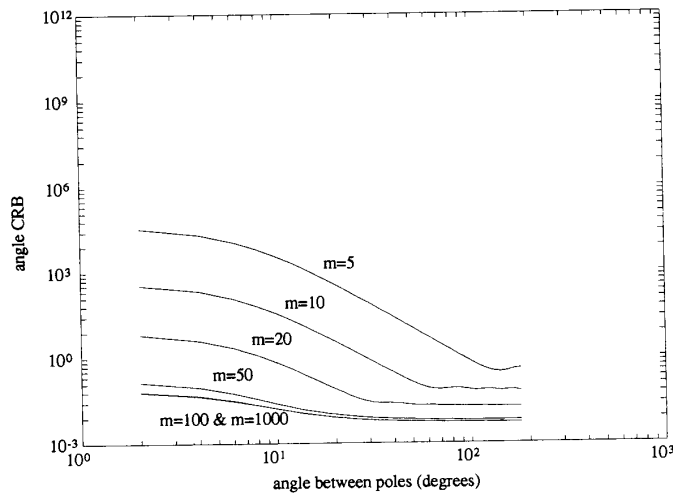


Fig. 7. Angle CRB for pole  $p_2$  as a function of angle separation, when  $\alpha_1 = 0.85$ ,  $\alpha_2 = 0.95$ .

*C. Some General Observations*

Using the CRB covariance matrix, one can determine a confidence region corresponding to an estimate of each pole. This region can be plotted as, for example, a CRB two standard deviation confidence "ellipse" about each pole. Fig. 8 is an example of such a plot. In this experiment there are ten poles, each with an energy of one. Here,  $m = 100$  data points and the noise power is  $\sigma = 0.1$ . The ellipses shown in Fig. 8 (they are actually circles, by Corollaries 1.a and 1.b) represent the two standard deviation concentration ellipses around the ten pole locations. If an efficient estimator is used, 87% of poles found in a Monte-Carlo simulation would be expected to fall within these circles. Note that the bounds are significantly smaller for the poles which are located close to the unit circle.

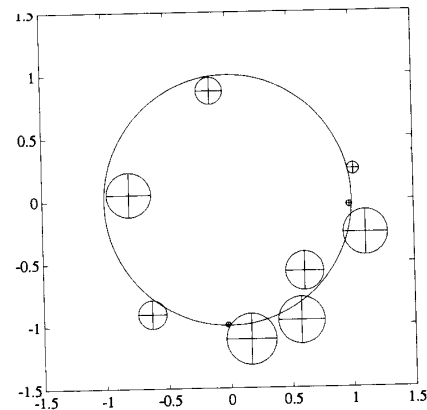


Fig. 8. Two standard deviation bounding circles for each pole, using a tenth-order model, with  $m = 100$  data points,  $\sigma = 0.1$ , and each mode energy set to unity.

These examples have confirmed the proven properties the CRB's, as well as suggesting the logarithmic symmetry of the CRB's for pole angle and relative magnitude. These properties give insight into how particular models affect the estimation of their parameters. We can see, for example, that the poles of equal energy modes can be better estimated when they are closer to the unit circle.

## V. CONCLUSIONS

In this paper we have provided complete expressions for the CRB of the parameters of an exponential model with one set of poles and multiple sets of amplitude coefficients. The poles of this model may lie anywhere in the complex plane. The CRB for the poles have been derived in terms of both rectangular and polar coordinate parameters. Using these expressions several useful properties of the CRB covariance matrices were established. It was proven that the polar and relative polar CRB's and some of the rectangular CRB's are independent of the absolute phase of the set of poles and each set of amplitude coefficients. In rectangular parameters it was proven that the real and imaginary part CRB's for both poles and amplitude coefficients are equal and uncorrelated. In polar coordinates the angle and magnitude CRB's were also proven to be uncorrelated; furthermore, the CRB's of the relative magnitudes and angles were shown to be equal. The examples presented support these properties as well as the fact that the CRB's of the pole angles and relative magnitudes are logarithmically symmetric about the unit circle. These results are useful for the analysis of parameter estimation methods. The CRB's themselves provide lower variance performance bounds for unbiased estimation, while the properties established give insight into how particular models will affect parameter estimation (e.g., pole locations).

## APPENDIX A PROOF OF THEOREM 1

First, we calculate the partial derivatives of (6) with respect to  $\sigma$ ,  $\{\bar{x}(t)\}$ ,  $\{\bar{y}(t)\}$ ,  $\{\bar{p}_i\}$ , and  $\{\bar{p}_i\}$ , which gives the following:

$$\frac{\partial \ln(L)}{\partial \sigma} = -\frac{mN}{\sigma} + \frac{1}{\sigma^2} \sum_{t=1}^N e^H(t) e(t) \quad (21)$$

$$\frac{\partial \ln(L)}{\partial \bar{x}(t)} = \frac{1}{\sigma} [A^H e(t) + A^T e^*(t)] = \frac{2}{\sigma} \operatorname{Re} \{A^H e(t)\} \quad (22)$$

$$\frac{\partial \ln(L)}{\partial \bar{y}(t)} = \frac{1}{\sigma} [-jA^H e(t) + jA^T e^*(t)] = \frac{2}{\sigma} \operatorname{Im} \{A^H e(t)\} \quad (23)$$

$$\frac{\partial \ln(L)}{\partial \bar{p}_i} = \frac{2}{\sigma} \sum_{t=1}^N \operatorname{Re} \left\{ x^H(t) \frac{dA^H}{d\bar{p}_i} e(t) \right\} \quad (24)$$

$$\frac{\partial \ln(L)}{\partial \bar{p}_i} = \frac{2}{\sigma} \sum_{t=1}^N \operatorname{Re} \left\{ x^H(t) \frac{dA^H}{d\bar{p}_i} e(t) \right\} \quad (25)$$

Defining  $\bar{p} = [\bar{p}_1 \bar{p}_2 \cdots \bar{p}_n]^T$  and  $\bar{p} = [\bar{p}_1 \bar{p}_2 \cdots \bar{p}_n]^T$  and carrying out the differentiation, (24) and (25) can be written compactly as

$$\frac{\partial \ln(L)}{\partial \bar{p}} = \frac{2}{\sigma} \sum_{t=1}^N \operatorname{Re} \{X^H(t) T_p^H A^H C e(t)\} \quad (26)$$

$$\frac{\partial \ln(L)}{\partial \bar{p}} = \frac{2}{\sigma} \sum_{t=1}^N \operatorname{Im} \{X^H(t) T_p^H A^H C e(t)\}. \quad (27)$$

From these results, the Fisher information matrix can be found as follows:

$$I_{\theta}^{\text{rect}} = E [\psi_{\theta}^{\text{rect}} \psi_{\theta}^{\text{rect}T}] \quad (28)$$

where the  $E[\cdot]$  denotes expectation and  $\psi_{\theta}^{\text{rect}T}$  is given by

$$\psi_{\theta}^{\text{rect}T} = \frac{\partial \ln(L)}{\partial \theta^{\text{rect}T}}. \quad (29)$$

To perform these expectations we need several results which are proven in [1]:

$$E[e^H(t) e(t) e^H(s) e(s)] = \begin{cases} m^2 \sigma^2 & \text{for } t \neq s \\ m(m-1) \sigma^2 & \text{for } t = s \end{cases} \quad (30)$$

$$E[e^H(t) e(t) e^T(s)] = 0 \quad \forall t, s \quad (31)$$

$$\operatorname{Re} \{x\} \operatorname{Re} \{y^T\} = \frac{1}{2} [\operatorname{Re} \{xy^T\} + \operatorname{Re} \{xy^H\}]$$

$$\operatorname{Im} \{x\} \operatorname{Im} \{y^T\} = -\frac{1}{2} [\operatorname{Re} \{xy^T\} - \operatorname{Re} \{xy^H\}]$$

$$\operatorname{Re} \{x\} \operatorname{Im} \{y^T\} = \frac{1}{2} [\operatorname{Im} \{xy^T\} + \operatorname{Im} \{xy^H\}]. \quad (32)$$

Using (30) we get

$$\begin{aligned} E \left[ \left( \frac{\partial \ln(L)}{\partial \sigma} \right)^2 \right] &= \frac{m^2 N^2}{\sigma^2} - 2 \frac{mN}{\sigma^3} \sum_{t=1}^N E[e^H(t) e(t)] \\ &\quad + \frac{1}{\sigma^4} \sum_{t=1}^N \sum_{s=1}^N E[e^H(t) e(t) e^H(s) e(s)] \\ &= \frac{m^2 N^2}{\sigma^2} - 2 \frac{m^2 N^2}{\sigma^2} + \frac{Nm}{\sigma^2} \\ &\quad \cdot [(N-1)m + (m+1)] \\ &= \frac{mN}{\sigma^2}. \end{aligned} \quad (33)$$

From (31), we see that  $\partial \ln(L)/\partial \sigma$  is not correlated with any of the other partial derivatives.

Next, we use (32) and the fact that  $E[e(t) e^T(s)] = 0 \quad \forall t, s$ , to obtain the following:

$$\begin{aligned} E \left[ \left( \frac{\partial \ln(L)}{\partial \bar{x}(t)} \right) \left( \frac{\partial \ln(L)}{\partial \bar{x}(s)} \right)^T \right] \\ = \frac{2}{\sigma} \operatorname{Re} \{A^H A\} \delta_{t,s} \end{aligned}$$

$$\begin{aligned} E \left[ \left( \frac{\partial \ln(L)}{\partial \bar{y}(t)} \right) \left( \frac{\partial \ln(L)}{\partial \bar{y}(s)} \right)^T \right] \\ = -\frac{2}{\sigma} \operatorname{Im} \{A^H A\} \delta_{t,s} \end{aligned}$$

$$E \left[ \left( \frac{\partial \ln(L)}{\partial \bar{x}(t)} \right) \left( \frac{\partial \ln(L)}{\partial \bar{p}} \right)^T \right] = \frac{2}{\sigma} \operatorname{Re} \{ A^H \operatorname{CAT}_p X(t) \}$$

$$E \left[ \left( \frac{\partial \ln(L)}{\partial \bar{x}(t)} \right) \left( \frac{\partial \ln(L)}{\partial \bar{p}} \right)^T \right] = -\frac{2}{\sigma} \operatorname{Im} \{ A^H \operatorname{CAT}_p X(t) \}$$

$$E \left[ \left( \frac{\partial \ln(L)}{\partial \bar{x}(t)} \right) \left( \frac{\partial \ln(L)}{\partial \bar{x}(s)} \right)^T \right] = \frac{2}{\sigma} \operatorname{Re} \{ A^H A \} \delta_{t,s}$$

$$E \left[ \left( \frac{\partial \ln(L)}{\partial \bar{p}} \right) \left( \frac{\partial \ln(L)}{\partial \bar{p}} \right)^T \right] = -\frac{2}{\sigma} \sum_{t=1}^N \operatorname{Im} \{ X^H(t) T_p^H A^H \operatorname{CCAT}_p X(t) \}$$

$$E \left[ \left( \frac{\partial \ln(L)}{\partial \bar{p}} \right) \left( \frac{\partial \ln(L)}{\partial \bar{p}} \right)^T \right] = \frac{2}{\sigma} \sum_{t=1}^N \operatorname{Re} \{ X^H(t) T_p^H A^H \operatorname{CCAT}_p X(t) \}. \quad (34)$$

Using the results of (34) in (28) and the variable substitutions of (9) we can see that the Fisher information matrix for the parameters in  $\theta^{\text{rect}}$  is given by (8).

In order to invert the real matrix  $I_{\theta}^{\text{rect}}$  to arrive at  $\operatorname{CRB}_{\theta}^{\text{rect}}$  we need the following lemma.

*Lemma A:* Assume we are given a real block matrix of the following form:

$$B' = \begin{bmatrix} \bar{B}(1, 1) & -\bar{B}(1, 1) & \cdots & \bar{B}(1, b) & -\bar{B}(1, b) \\ \bar{B}(1, 1) & \bar{B}(1, 1) & \cdots & \bar{B}(1, b) & \bar{B}(1, b) \\ \vdots & \vdots & \ddots & \vdots & \vdots \\ \bar{B}(b, 1) & -\bar{B}(b, 1) & \cdots & \bar{B}(b, b) & -\bar{B}(b, b) \\ \bar{B}(b, 1) & \bar{B}(b, 1) & \cdots & \bar{B}(b, b) & \bar{B}(b, b) \end{bmatrix}. \quad (35)$$

Then the  $B'^{-1}$  is given by

$$B'^{-1} = \begin{bmatrix} \bar{B}'(1, 1) & -\bar{B}'(1, 1) & \cdots & \bar{B}'(1, b) & -\bar{B}'(1, b) \\ \bar{B}'(1, 1) & \bar{B}'(1, 1) & \cdots & \bar{B}'(1, b) & \bar{B}'(1, b) \\ \cdots & \vdots & \ddots & \vdots & \vdots \\ \bar{B}'(b, 1) & -\bar{B}'(b, 1) & \cdots & \bar{B}'(b, b) & -\bar{B}'(b, b) \\ \bar{B}'(b, 1) & \bar{B}'(b, 1) & \cdots & \bar{B}'(b, b) & \bar{B}'(b, b) \end{bmatrix}. \quad (36)$$

$$E \left[ \left( \frac{\partial \ln(L)}{\partial \bar{x}(t)} \right) \left( \frac{\partial \ln(L)}{\partial \bar{p}} \right)^T \right] = \frac{2}{\sigma} \operatorname{Im} \{ A^H \operatorname{CAT}_p X(t) \}$$

$$E \left[ \left( \frac{\partial \ln(L)}{\partial \bar{x}(t)} \right) \left( \frac{\partial \ln(L)}{\partial \bar{p}} \right)^T \right] = \frac{2}{\sigma} \operatorname{Re} \{ A^H \operatorname{CAT}_p X(t) \}$$

$$E \left[ \left( \frac{\partial \ln(L)}{\partial \bar{p}} \right) \left( \frac{\partial \ln(L)}{\partial \bar{p}} \right)^T \right] = \frac{2}{\sigma} \sum_{t=1}^N \operatorname{Re} \{ X^H(t) T_p^H A^H \operatorname{CCAT}_p X(t) \}$$

where  $B' = B^{-1}$  and where  $B$  and  $B'$  are given by the following block matrices:

$$B = \begin{bmatrix} B(1, 1) & \cdots & B(1, b) \\ \vdots & \ddots & \vdots \\ B(b, 1) & \cdots & B(b, b) \end{bmatrix}$$

$$B' = \begin{bmatrix} B'(1, 1) & \cdots & B'(1, b) \\ \vdots & \ddots & \vdots \\ B'(b, 1) & \cdots & B'(b, b) \end{bmatrix}. \quad (37)$$

*Proof:* Note that  $B$  can be written in the following

form:

$$\begin{aligned}
 B^r &= T_B \begin{bmatrix} \bar{B}(1,1) \cdots \bar{B}(1,b) & -\bar{B}(1,1) \cdots -\bar{B}(1,b) \\ \vdots & \vdots \\ \bar{B}(b,1) \cdots \bar{B}(b,b) & -\bar{B}(b,1) \cdots -\bar{B}(b,b) \\ \bar{B}(1,1) \cdots \bar{B}(1,b) & \bar{B}(1,1) \cdots \bar{B}(1,b) \\ \vdots & \vdots \\ \bar{B}(b,1) \cdots \bar{B}(b,b) & \bar{B}(b,1) \cdots \bar{B}(b,b) \end{bmatrix} T_B \\
 &= T_B \begin{bmatrix} \bar{B} & -\bar{B} \\ \bar{B} & \bar{B} \end{bmatrix} T_B
 \end{aligned} \tag{38}$$

where  $T_B$  is given by

$$T_B = \begin{bmatrix} & & & 1 & & & \\ & & & & \ddots & & \\ & & & & & & \\ 1 & & & & & & \\ & & & & & & \\ & & & & & & \\ & & & & & & \\ & & & & & & 1 \end{bmatrix} \tag{39}$$

Since  $T_B^{-1} = T_B$  and since

$$\begin{bmatrix} \bar{B} & -\bar{B} \\ \bar{B} & \bar{B} \end{bmatrix}^{-1} = \begin{bmatrix} \bar{B}' & -\bar{B}' \\ \bar{B}' & \bar{B}' \end{bmatrix}$$

(see [1]), the inverse of  $B^r$  is given by

$$B^{r-1} = T_B \begin{bmatrix} \bar{B}' & -\bar{B}' \\ \bar{B}' & \bar{B}' \end{bmatrix} T_B \tag{40}$$

which is the same as the expression given by (36).  $\square$

Using Lemma A we note that we can obtain  $\text{CRB}_\theta^{\text{rect}}$  by inverting the following complex matrix:

$$\tilde{I}_\theta^{\text{rect}} = \begin{bmatrix} \frac{mN}{\sigma^2} & & & & & \\ & Q & & & R(1) & \\ & & \ddots & & \vdots & \\ & & & & Q & R(N) \\ R^H(1) \cdots R^H(N) & & & & & S \end{bmatrix} \tag{41}$$

Using the matrix inversion lemma and the definitions on (12) we can see that the inverse is given by

$$\text{CRB}_\theta^{\text{rect}} = \begin{bmatrix} \frac{\sigma^2}{mN} & & & & & \\ & Q'(1,1) \cdots Q'(1,N) & R'(1) & & & \\ & \vdots & \vdots & & & \\ & Q'(N,1) \cdots Q'(N,N) & R'(N) & & & \\ R^H(1) \cdots R^H(N) & & & S' & & \end{bmatrix} \tag{42}$$

We now note that this complex matrix corresponds to the real CRB matrix given by (11).  $\square$

#### APPENDIX B PROOF OF THEOREM 2

The proof is similar to that of Theorem 1 and only the differences will be noted here. We calculate the partial derivatives of (6) with respect to  $\sigma$ ,  $\{\gamma(t)\}$ ,  $\{\beta(t)\}$ ,  $\{\omega_i\}$ , and  $\{\alpha_i\}$ . Thus (22), (23), (26), and (27) are replaced by

$$\begin{aligned}
 \frac{\partial \ln(L)}{\partial \gamma(t)} &= \frac{2}{\sigma} \text{Im} \{ X^H(t) A^H e(t) \} \\
 \frac{\partial \ln(L)}{\partial \beta(t)} &= \frac{2}{\sigma} \text{Re} \{ X^H(t) T_\beta(t) A^H e(t) \} \\
 \frac{\partial \ln(L)}{\partial \omega} &= \frac{2}{\sigma} \sum_{t=1}^N \text{Im} \{ X^H(t) A^H C e(t) \} \\
 \frac{\partial \ln(L)}{\partial \alpha} &= \frac{2}{\sigma} \sum_{t=1}^N \text{Re} \{ X^H(t) T_\alpha A^H C e(t) \}
 \end{aligned} \tag{43}$$

where  $\omega = [\omega_1 \ \omega_2 \ \cdots \ \omega_n]^T$  and  $\alpha = [\alpha_1 \ \alpha_2 \ \cdots \ \alpha_n]^T$ .

From these results, the Fisher information matrix can be found as follows:

$$I_\theta^{\text{pol}} = E[\psi_\theta^{\text{pol}} \psi_\theta^{\text{pol}T}] \tag{44}$$

where  $\psi_\theta^{\text{pol}T}$  is given by

$$\psi_\theta^{\text{pol}T} = \frac{\partial \ln(L)}{\partial \theta^{\text{pol}T}} \tag{45}$$

The expressions in (34) are thus replaced by

$$\begin{aligned}
 &E \left[ \left( \frac{\partial \ln(L)}{\partial \gamma(t)} \right) \left( \frac{\partial \ln(L)}{\partial \gamma(s)} \right)^T \right] \\
 &= \frac{2}{\sigma} \text{Re} \{ X^H(t) A^H A X(s) \} \delta_{t,s} \\
 &E \left[ \left( \frac{\partial \ln(L)}{\partial \gamma(t)} \right) \left( \frac{\partial \ln(L)}{\partial \beta(s)} \right)^T \right] \\
 &= \frac{2}{\sigma} \text{Im} \{ X^H(t) A^H A T_\beta(s) X(s) \} \delta_{t,s}
 \end{aligned}$$

$$\begin{aligned}
 & E \left[ \left( \frac{\partial \ln(L)}{\partial \gamma(t)} \right) \left( \frac{\partial \ln(L)}{\partial \omega} \right)^T \right] \\
 &= \frac{2}{\sigma} \operatorname{Re} \{ X^H(t) A^H C A X(t) \} \\
 & E \left[ \left( \frac{\partial \ln(L)}{\partial \gamma(t)} \right) \left( \frac{\partial \ln(L)}{\partial \alpha} \right)^T \right] \\
 &= \frac{2}{\sigma} \operatorname{Im} \{ X^H(t) A^H C A T_\alpha X(t) \} \\
 & E \left[ \left( \frac{\partial \ln(L)}{\partial \beta(t)} \right) \left( \frac{\partial \ln(L)}{\partial \beta(s)} \right)^T \right] \\
 &= \frac{2}{\sigma} \operatorname{Re} \{ X^H(t) T_\beta(t) A^H A T_\beta(s) X(s) \} \delta_{t,s} \\
 & E \left[ \left( \frac{\partial \ln(L)}{\partial \beta(t)} \right) \left( \frac{\partial \ln(L)}{\partial \omega} \right)^T \right] \\
 &= -\frac{2}{\sigma} \operatorname{Im} \{ X^H(t) T_\beta(t) A^H C A X(t) \} \\
 & E \left[ \left( \frac{\partial \ln(L)}{\partial \beta(t)} \right) \left( \frac{\partial \ln(L)}{\partial \alpha} \right)^T \right] \\
 &= \frac{2}{\sigma} \operatorname{Re} \{ X^H(t) T_\beta(t) A^H C A T_\alpha X(t) \} \\
 & E \left[ \left( \frac{\partial \ln(L)}{\partial \omega} \right) \left( \frac{\partial \ln(L)}{\partial \omega} \right)^T \right] \\
 &= \frac{2}{\sigma} \sum_{t=1}^N \operatorname{Re} \{ X^H(t) A^H C C A X(t) \} \\
 & E \left[ \left( \frac{\partial \ln(L)}{\partial \omega} \right) \left( \frac{\partial \ln(L)}{\partial \alpha} \right)^T \right] \\
 &= \frac{2}{\sigma} \sum_{t=1}^N \operatorname{Im} \{ X^H(t) A^H C C A T_\alpha X(t) \} \\
 & E \left[ \left( \frac{\partial \ln(L)}{\partial \alpha} \right) \left( \frac{\partial \ln(L)}{\partial \alpha} \right)^T \right] \\
 &= \frac{2}{\sigma} \sum_{t=1}^N \operatorname{Re} \{ X^H(t) T_\alpha A^H C C A T_\alpha X(t) \}. \quad (46)
 \end{aligned}$$

Using the results of (46) in (44), the variable substitutions of (14), and the fact that the matrices  $T_\beta(t)$  and  $T_\alpha$  are diagonal and can thus be commuted with the diagonal matrices  $X(t)$  and subsequently factored out we can see that the Fisher information matrix for the parameters in  $\theta^{\text{pol}}$  is given by (13).

In order to invert the real matrix  $I_\theta^{\text{pol}}$  to arrive at  $\text{CRB}_\theta^{\text{pol}}$  we first note that it can be written as (cf. Theorem 3)

$$I_\theta^{\text{pol}} = J^H I_\theta^{\text{relpol}} J \quad (47)$$

where  $J$  is the block diagonal matrix given by

$$J = \text{diag} \{ I_n, T_\beta(1), I_n, T_\beta(2), \dots, I_n, T_\beta(N), I_n, T_\alpha \}. \quad (48)$$

Thus  $\text{CRB}_\theta^{\text{pol}}$  is given by

$$\text{CRB}_\theta^{\text{pol}} = J^{-1} I_\theta^{\text{relpol}^{-1}} J^{-1}. \quad (49)$$

The inverses involving  $J$  are straightforward since it is a diagonal matrix.

Using the expression for  $[I_\theta^{\text{relpol}}]^{-1}$  from Theorem 3, which is derived in Appendix C, in (49), and performing the multiplication we obtain the CRB matrix by (16).  $\square$

#### APPENDIX C PROOF OF THEOREM 3

The proof is obtained by noting that the relative polar parameterization is simply a scaling transformation of the absolute polar parameterization using the transformation matrix  $J$  (cf. Appendix B) as follows:

$$I_\theta^{\text{relpol}} = J^{-1} I_\theta^{\text{pol}} J^{-1} \quad (50)$$

from which we can see that  $I_\theta^{\text{relpol}}$  is given by (19).

Using Lemma A we can obtain the result for  $\text{CRB}_\theta^{\text{relpol}}$  by inverting the following complex matrix:

$$\bar{I}_\theta^{\text{relpol}} = \begin{bmatrix} \frac{mN}{\sigma^2} & & & & & \\ & U(1) & & & & V(1) \\ & & \ddots & & & \vdots \\ & & & & U(N) & V(N) \\ & & & & & \\ & & & & V^H(1) \cdots V^H(N) & W \end{bmatrix}. \quad (51)$$

Using the matrix inversion lemma and the definitions in (12) we can see that the inverse is given by

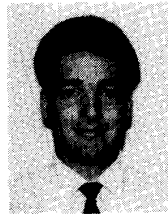
$$\text{CRB}_\theta^{\text{relpol}} = \begin{bmatrix} \frac{\sigma^2}{mN} & & & & & \\ & U'(1,1) \cdots U'(1,N) & & & & V'(1) \\ & \vdots & \ddots & \vdots & & \vdots \\ & & & & U'(N,1) \cdots U'(N,N) & V'(N) \\ & & & & & \\ & & & & V'^H(1) \cdots V'^H(N) & W' \end{bmatrix}$$

from which we can see that  $\text{CRB}_\theta^{\text{relpol}}$  is given by (20).  $\square$

#### REFERENCES

- [1] P. Stoica and A. Nehorai, "MUSIC, maximum likelihood, and Cramer-Rao bound," *IEEE Trans. Acoust., Speech, Signal Processing*, vol. 37, pp. 720-741, May 1989.
- [2] Y. Hua and T. K. Sarker, "A perturbation property of the TLS-LP method," *IEEE Trans. Acoust., Speech, Signal Processing*, vol. 38, pp. 2004-2005, Nov. 1990.
- [3] R. Kumaresan and D. W. Tufts, "Estimating the parameters of exponentially damped sinusoids and pole-zero modeling in noise," *IEEE Trans. Acoust., Speech, Signal Processing*, vol. ASSP-30, pp. 833-840, Dec. 1982.

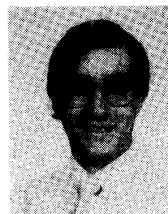
- [4] R. O. Schmidt, "Multiple emitter location and signal parameter estimation," in *Proc. RADC Spectral Estimation Workshop*, Rome, NY, 1979, pp. 243-258.
- [5] R. Roy, A. Paulraj, and T. Kailath, "ESPRIT—a subspace rotation approach to estimation of parameters of cisoids in noise," *IEEE Trans. Acoust., Speech, Signal Processing*, vol. ASSP-34, pp. 1340-1342, Apr. 1986.
- [6] Y. Bresler and A. Macovski, "Exact maximum likelihood parameter estimation of superimposed exponential signals in noise," *IEEE Trans. Acoust., Speech, Signal Processing*, vol. ASSP-34, pp. 1361-1375, Oct. 1986.
- [7] R. Kumaresan, L. L. Scharf, and A. K. Shaw, "An algorithm for pole-zero modeling and analysis," *IEEE Trans. Acoust., Speech, Signal Processing*, vol. ASSP-34, pp. 637-640, June 1986.
- [8] M. Kaveh and A. J. Barabell, "The statistical performance of the MUSIC and the minimum-norm algorithms in resolving plane waves in noise," *IEEE Trans. Acoust., Speech, Signal Processing*, vol. ASSP-34, pp. 331-341, Apr. 1986.
- [9] M. A. Rahman and K.-B. Yu, "Total least squares approach for frequency estimation using linear prediction," *IEEE Trans. Acoust., Speech, Signal Processing*, vol. ASSP-35, pp. 1440-1454, Oct. 1987.
- [10] I. Ziskind and M. Wax, "Maximum likelihood localization of multiple sources by alternating projection," *IEEE Trans. Acoust., Speech, Signal Processing*, vol. 36, pp. 1553-1560, Oct. 1988.
- [11] R. Roy and T. Kailath, "ESPRIT—estimation of signal parameters via rotational invariance techniques," *IEEE Trans. Acoust., Speech, Signal Processing*, vol. 37, pp. 984-995, July 1989.
- [12] M. D. Zoltowski and D. Stavrinos, "Sensor array signal processing via a Procrustes rotations based on eigenanalysis of the ESPRIT data pencil," *IEEE Trans. Acoust., Speech, Signal Processing*, vol. 37, pp. 832-861, June 1989.
- [13] Y. Hua and T. K. Sarker, "Matrix pencil method for estimating parameters of exponentially damped/undamped sinusoids in noise," *IEEE Trans. Acoust., Speech, Signal Processing*, vol. 38, pp. 814-824, May 1990.
- [14] T. J. Abatzoglou and L. K. Lam, "Direction finding using uniform arrays and the constrained total least squares method," in *Proc. Twenty-Fifth Asilomar Conf. Signals, Syst., Comput.*, Pacific Grove, CA, Nov. 4-6, 1991.
- [15] W. M. Steedly and R. L. Moses, "High resolution exponential modeling of fully polarized radar returns," *IEEE Trans. Aerosp. Electron. Syst.*, vol. 27, pp. 459-469, May 1991.
- [16] D. C. Rife and R. R. Boorstyn, "Multiple tone parameter estimation from discrete-time observations," *Bell Syst. Tech. J.*, vol. 55, pp. 1389-1410, Nov. 1976.
- [17] G. R. L. Sohie, G. N. Maracas, and A. Mirchandani, "Estimation of decay rates of transient signals," *IEEE Trans. Acoust., Speech, Signal Processing*, vol. 38, pp. 370-372, Feb. 1990.



**William M. Steedly** (S'86-M'93) received the B.S. degree in electrical engineering from Virginia Polytechnic Institute and State University, Blacksburg, in 1988 and the M.S. and Ph.D. degrees in electrical engineering from the Ohio State University, Columbus, in 1989 and 1992, respectively.

During the 1988-1989 academic year he was an Ohio State University Fellow. During the 1989-1992 academic years he was an Air Force Laboratory Graduate Fellow in the Department of Electrical Engineering, Ohio State University. He spent the summer of 1990 at Wright Labs, Wright Patterson AFB, OH. He is currently a member of the Technical Staff of the Analytic Sciences Corporation, Reston, VA. His primary research interests are in digital signal processing, and include parametric modeling techniques and their application to radar signal processing.

Dr. Steedly is a member of Eta Kappa Nu, Tau Beta Pi, Phi Kappa Phi, and Sigma Xi.



**Randolph L. Moses** (S'78-M'83-SM'90) received the B.S., M.S., and Ph.D. degrees in electrical engineering from Virginia Polytechnic Institute and State University in 1979, 1980, and 1984, respectively.

During the summer of 1983 he was a SCEE Summer Faculty Research Fellow at Rome Air Development Center, Rome, NY. From 1984 to 1985 he was with the Eindhoven University of Technology, Eindhoven, The Netherlands, as a NATO Postdoctoral Fellow. Since 1985 he has

been with the Department of Electrical Engineering, Ohio State University, and is currently an Associate Professor there. His research interests are in digital signal processing, and include parametric time series analysis, radar signal processing, system identification, and model reduction.

Dr. Moses is a member of Eta Kappa Nu, Tau Beta Pi, Phi Kappa Phi, and Sigma Xi.